Nuclear Instruments and Methods in Physics Research B 291 (2012) 65–72

Contents lists available at SciVerse ScienceDirect

Nuclear Instruments and Methods in Physics Research B

journal homepage: www.elsevier.com/locate/nimb

Thermoluminescence characteristics of the novel CaF_2:Dy nanoparticles prepared by using the hydrothermal method

M. Zahedifar [a,b,*], E. Sadeghi [a], S. Harooni [a]

[a] Physics Department, University of Kashan, Kashan, Iran
[b] Institute of Nanoscience and Nanotechnology, University of Kashan, Kashan, Iran

ARTICLE INFO

Article history:
Received 30 March 2012
Received in revised form 12 September 2012
Available online 27 September 2012

Keywords:
Thermoluminescence
CaF_2:Dy
Nanoparticles
Hydrothermal

ABSTRACT

Dysprosium doped calcium fluoride (CaF_2:Dy) nanoparticles were produced for the first time by using the hydrothermal method. X-ray diffraction (XRD), scanning electron microscope (SEM) and energy dispersive spectrometer (EDS) patterns were utilized to characterize the synthesized material. The particle size of about 43 nm was evaluated from XRD data and supported by the SEM images. The $T_m - T_{stop}$ and the computerized glow curve de-convolution (CGCD) methods were employed to determine the number of component glow peaks and kinetic parameters of the synthesized nanoparticles. Thermoluminescence glow curve of this phosphor exhibits six overlapping glow peaks. The optimized concentration of Dy impurity was found at 3 mol%. The prepared nanoparticles exhibit a roughly linear dose response to absorbed dose of 1000 Gy received from ^{60}Co gamma source. This finding recommends this nanomaterial as a good candidate for high dose dosimetry. Other dosimetric features of this novel phosphor are also presented and discussed.

1. Introduction

Monitoring of radiation dose is of vital importance in all branches where ionizing radiation is used. Thermoluminescence (TL) is a radiation dosimetric method that is widely used to personal, environmental and clinical dosimetry. The peak area and the peak intensity of a TL dosimeter are proportional to the received dose from the radiation field. Amongst the widely used commercial microcrystalline TL phosphors, calcium fluoride doped with dysprosium, known as TLD-200, has a TL sensitivity of about 10–30 times greater than that of LiF:Mg,Ti (TLD-100) [1]. Therefore this phosphor has found extensive applications in the personal and environmental dosimetry [2]. In addition, this phosphor is capable of being applied for the mixed field dosimetry and estimating the different dose components as the peak height ratios of this TL material is correlated to the type of the radiation field [3]. The relative neutron sensitivity of CaF_2:Dy is more than CaF_2:Mn and less than CaF_2:T_m and it increases with increase in the neutron energy [4]. Different numbers of 5–9 peak components have been reported for the complex glow curve of CaF_2:Dy microcrystalline [5–7]. In recent years, nanomaterials in various fields of pure and applied sciences have attracted a great deal of interest amongst the researchers. The optical properties of nanostructures, depend strongly on their dimensions and can be very different from those of their bulk equivalent. Recently, many researches have been devoted to the TL properties of different nanomaterials that show some outstanding characteristics for instance high sensitivity and saturation at very high dose levels [8–14]. It has been found that the size of the pure nanomaterials of calcium fluoride synthesized by the co-precipitation method is larger than those produced using the hydrothermal method [15]. The Eu, Er and Yb doped CaF_2 nanoparticles have also been synthesized [16,17] and very recently the preparation method and TL characteristics of CaF_2:Mn nanoparticles has been reported [18]. Considering the extensive applications of the microcrystalline CaF_2:Dy in TL dosimetry, investigation of TL characteristics of its nanoscale counterpart is of importance. In this work, the synthesis process of CaF_2:Dy nanoparticles prepared by using the hydrothermal method is explained and TL dosimetric features of this novel nanostructure are presented and discussed.

2. Experimental procedure

2.1. The hydrothermal method of preparation

CaF_2:Dy nanoparticles were prepared with the hydrothermal method based on the following reaction:

$$Ca(NO_3)_2 + 2NH_4F \rightarrow CaF_2 + 2NH_4(NO_3)$$

The raw materials used for synthesis of this phosphor were $Ca(NO_3)_2$ (of 99.95% purity), NH_4F (of 99.9% purity), $Dy(NO_3)_3$ (of 99.99% purity), Brij 35 (of 99.9% purity), distilled de-ionized water

* Corresponding author at: Physics Department, University of Kashan, Kashan, Iran. Tel.: +98 361 5559931; fax: +98 361 5552930.
E-mail address: zhdfr@kashanu.ac.ir (M. Zahedifar).

0168-583X/$ - see front matter © 2012 Elsevier B.V. All rights reserved.
http://dx.doi.org/10.1016/j.nimb.2012.09.013

and ethanol (Merck Chemical). first of all, 0.300 g of calcium nitrate was dissolved in a mixture of 15 cc deionized water and 15 cc ethanol and was stirred for 10 min. Then the solution of ammonium fluoride was prepared by dissolving 0.094 g NH_4F in a mixture of 40 cc ethanol and 20 cc distilled deionized water. 7.5 g of Brij 35 surfactant was dissolved in 30 cc deionized water and the resulting solution was placed on a stirrer until the Brij was solved completely. This solution of Brij was added slowly to the calcium nitrate solution (prepared in the first step) while was placed on a stirrer. Different amounts of dysprosium nitrate were added to the last mixture and finally NH_4F solution was appended slowly. The final mixture was placed in an autoclave at 200 °C for 12 h. Following cooling the product, the solid part was collected by centrifuging the mixture and was washed with de-ionized water for several times. The final CaF_2:Dy nanoparticles were obtained following drying the product in an oven for 2 h at 150 °C.

2.2. Sample analysis

The structural characteristics of the sample were supported by X-ray diffraction (XRD) with Rigaku D-maxcIII diffractometer using CuK_α radiation. SEM images were obtained using a scanning electron microscope model Philips XL-30 ESEM equipped with energy dispersive spectrometer (EDS). Photoluminescence (PL) spectrum was recorded using a Perkin–Elmer spectrometer model LS55 with photo multiplier tube and Xenon lamp at room temperature. All irradiations were made using a ^{60}Co gamma source. For the readout facility, a Harshaw TLD reader model 4500 was used. The heating rate applied for readout was 1 °C/s (with preheat of 50 °C) to a maximum temperature of 350 °C. The samples were annealed at 500 °C for 60 min using a programmable oven with temperature accuracy of ± 1 °C and then were cooled rapidly to room temperature (75 °C/min). Since the TL response depends on the mass of the sample, the masses were kept constant at 0.02 g with an accuracy of ± 0.01 mg. Because of light sensitivity of CaF_2:Dy, all experimental stages were performed in the dark.

3. Results

3.1. SEM, EDS, XRD and PL analyses

X-ray diffraction pattern of CaF_2:Dy nanoparticles is observed in Fig. 1. The sharp peaks were assigned to diffractions on (111), (220), (311), (400), (331) planes and two low intensity peaks were attributed to diffractions on (222) and (420) planes. These findings reveal that the sample is CaF_2 with cubic lattice structure and corresponds to ICSD collection code No. 060368. From XRD pattern, the crystalline size, D was estimated using the Scherrer's formula:

$$D = \frac{K\lambda}{\beta \cos\theta} \quad (1)$$

Where the constant k is 0.9, λ is the wavelength of CuK_α (1.540562 Å) line, β is the full width at half-maximum (FWHM) and θ, the diffraction angle. The crystalline sizes, D of CaF_2:Dy using the dominant (220) peak was calculated to be approximately 43 nm. In order to further reveal the size and the shape of the prepared CaF_2:Dy nanoparticles, the SEM images were utilized. The results are shown in Fig. 2. As is obvious, the scatter in the particle size is not considerable and the average dimension is in agreement with that calculated from Eq. (1). EDS spectrum of CaF_2:Dy nanoparticles is seen in Fig. 3. The element concentrations are inserted as inset of the figure. Two emission bands at 480 nm (blue emission peak) and 575 nm (yellow emission peak) of Dy^{3+} ion in bulk CaF_2:Dy can be attributed to transitions from $^4F_{9/2}$ to $^6H_{15/2}$ and $^6H_{13/2}$ respectively [19]. Fig. 4 shows the emission spectra of CaF_2: Dy nanoparticles. As is apparent, two strong blue and yellow emission bands at 479 and 574 nm exist in the PL emission. The weak blue shifting is a result of the quantum size effect, i.e. decrease in particle size, results in diminution of number of allowed transitions to some extent in the nanoparticles. Also many weaker satellite PL peaks are present in the emission spectra of the synthesized nanoparticles. The existence of these additive bands can be explained in the following way. It is well established that the nanoscale materials have large surface to volume ratio and the surface defects like Schottky and Frenkel exist in the lattice structure of alkali halides at all temperatures. These kinds of vacancies on the surface of nanoparticles cause the PL emission at different wavelengths.

3.2. Thermoluminescence properties

Finding an optimum pre-irradiation annealing regime for TL materials is of crucial importance in TL dosimetry. Therefore, the effects of annealing temperature and duration on TL characteristics of the synthesized nanoparticles were studied. It was found that the TL sensitivity of the produced nanoparticles vary for different applied annealing regimes. The optimum sensitivity was realized for thermal treatment of 500 °C for 60 min and this annealing regime was used for succeeding studies. In order to identify the number of glow peaks contained in the complex glow curve of the synthesized phosphor, the $T_m - T_{stop}$ method was employed. Heating the phosphors to T_{stop} causes a fraction of electrons to release from the trapping states, so in subsequent recording the glow curve, re-trapping probability increases and T_m (maximum temperature of the main peak) shifts to the higher temperatures and the number of emitted photons and intensity of the peak maximum decreases. All the samples were first annealed to a specific temperature (T_{stop}) with a constant heating rate of 3 °C/s , then were cooled rapidly to room temperature in nitrogen atmosphere and subsequently were heated in the TL reader with a heating rate of 2 °C/s for recording the glow curve. Fig. 5(a) shows the variation of T_m versus T_{stop} for the main peak of this phosphor following irradiating the samples with 10 Gy gamma rays by the ^{60}Co source. As is evident, increasing the T_{stop} from 80 °C to 300 °C causes the T_m to grow from 175 °C to 298 °C. However this increase is not monotonic and two jumps are observed. The first plateau zone in Fig. 5(a) can be attributed to a single glow peak, while the second and the third plateaus with relatively higher slopes inform us about overlapping glow peaks. The low temperature glow peak at approximately 125 °C did not contribute to Fig. 5(a) due to its very low intensity. The second plateau with higher slope which corresponds to the peak No.3 informs us about an overlap of closely lying glow peaks in the temperature range in which this plateau is appeared. For identifying the number of components constructing the glow peak 3 at about 500 K, the thermal cleaning method was first utilized to remove the two lower temperature glow peaks from the complex glow curve. Then the CGCD procedure was performed using different numbers of constituents for peak 3 as the input of the program and in each case the FOM value was used as the criterion for the correctness of the assumed number of peak components. In Fig. 6, the two glow peaks 3, 4 obtained following thermally removal of glow peaks 1 and 2 and high temperature glow peaks are shown with open circles. The lowest FOM value of 0.38 was obtained when three components were considered for peak 3. The slope of the second plateau in Fig. 5(a) can be understood considering the overlapping peaks 3a, 3b, and 3c in Fig.6. As is evident in Fig. 6, the glow peak 3a and 3c are located under the area of peak 3b. Furthermore, the

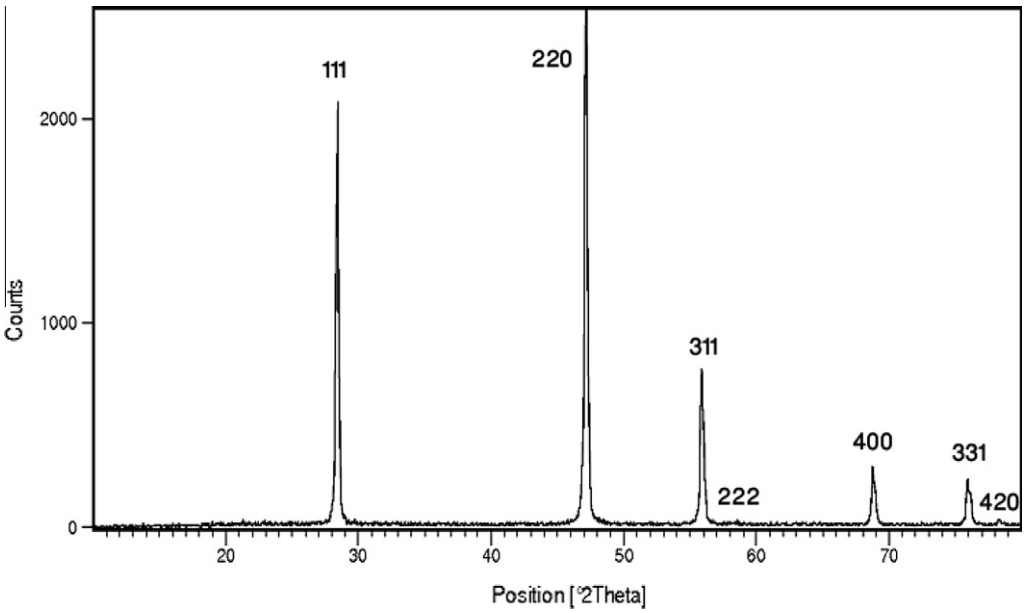

Fig. 1. XRD pattern of the synthesized CaF_2:Dy nanoparticles.

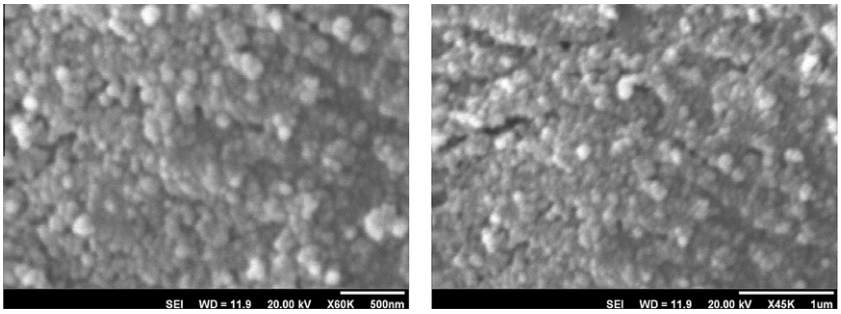

Fig. 2. SEM images of produced CaF_2:Dy nanoparticles.

glow peak 3a has very low intensity compared to the glow peaks 3b and 3c and the peak maximum temperatures of peak 3b and 3c are very close to each other. Hence in the plot of $T_m - T_{stop}$ for peak 3 we encountered a monotonic increase of T_m versus T_{stop} instead of discrete jumps of T_m. A discussion on the slope of the third plateau in the Fig. 5 which belongs to the last peak of this phosphor is in order. At first glance, an approximately high slope of this plateau informs about overlapping peaks. Fig. 5b shows an overlapping between the glow peak 4 at approximately 300 °C and the higher temperature glow peaks of this phosphor which causes the temperature of the peak maximum at about 300 °C to shift to higher temperatures with increase in the T_{stop}. As is shown in Fig. 6, the glow peak 4 is fairly fitted to a single glow peak when this glow peak is separated from the higher temperature peaks by using thermal cleaning method. Fig.7 shows the total glow curve of this phosphor and the constituent glow peaks. The difference between the intensity of the experimental glow curve and that obtained by adding the intensities of the fitted glow peaks is shown as residue at the top of the Fig.7. The FOM value of 0.70 indicates a good fit to the experimental glow curve. The kinetic parameters of the component glow peaks obtained by using the CGCD method are shown in the Table 1. Glow peaks were deconvolved using CGCD program, which was produced in our laboratory using the Levenberg–Marquart algorithm. This program uses the general order kinetics, the mixed order kinetics and complex functions describing the continuous trap distribution to parameterize the shape of the glow peaks. The TL intensity in general order kinetics model in terms of the intensity and the temperature of the peak maximum is given by [20]

$$I(T) = I_m b^{\frac{b}{b-1}} \exp\left(\frac{E(T-T_m)}{KTT_m}\right) \times \left\{\frac{T^2}{T_m^2}(b-1)\left(1-\frac{2KT}{E}\right)\exp\left(\frac{E(T-T_m)}{kTT_m}\right) + 1 + (b-1)\frac{2kT_m}{E}\right\}^{\frac{-b}{b-1}} \quad (2)$$

In which I_m is the maximum TL intensity, T_m (K) the maximum temperature, T (K) the absolute temperature, E (eV) the activation energy, k (eV/K) the Boltzmann constant and b the kinetic order. The free parameters of each TL glow peak in CGCD procedure are I_m, T_m, E and b. The used glow curve deconvolution function (in terms of I_m, T_m, E and b) has advantage over the deconvolution function in terms of n_o (initial concentration of electrons in trapping states), S (the pre exponential factor), E and b since I_m and T_m can easily be estimated from the experimental glow curve as the initial values for curve fitting procedure. Also the used function for general order kinetics is more useful than the deconvolution functions for the limiting cases of first and second- orders kinetics since intermediate cases in which $1 < b < 2$ can be dealt and it

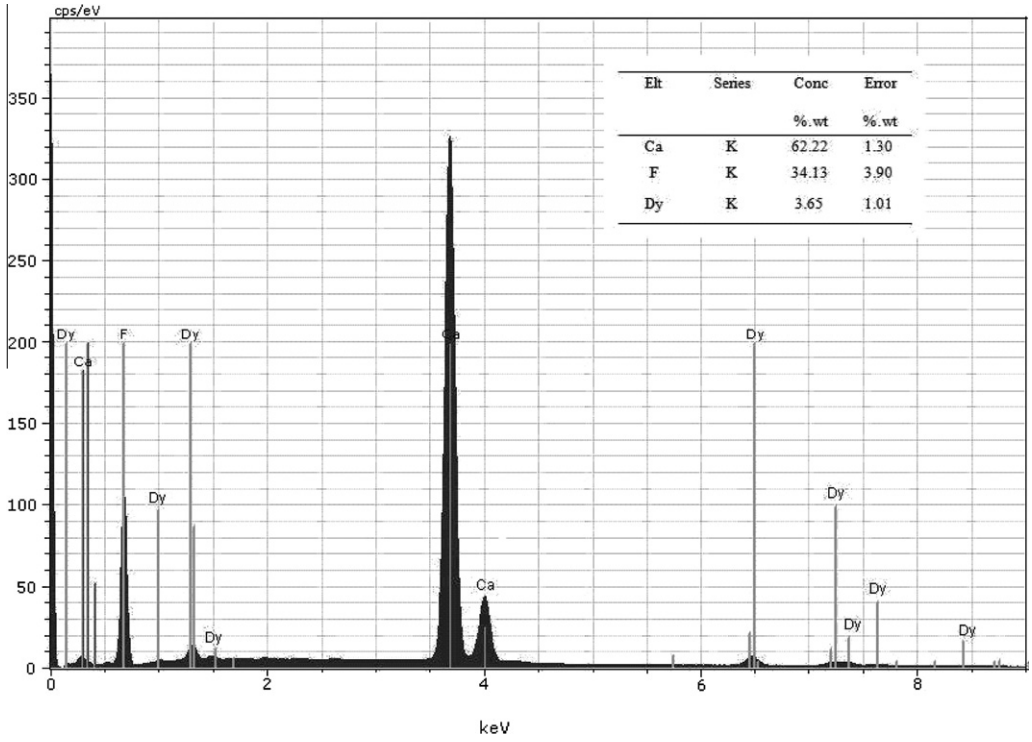

Fig. 3. EDS spectra of synthesized CaF_2:Dy nanoparticles at optimum concentration of 3 mol% of Dy. Inset of the figure shows further results of EDS analysis.

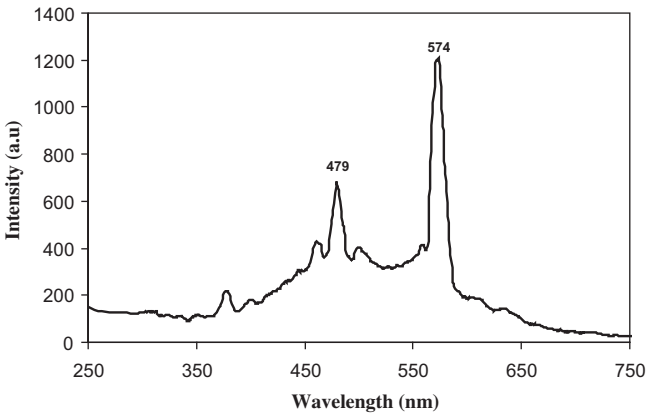

Fig. 4. Photoluminescence emission spectra of CaF_2:Dy nanoparticles.

smoothly goes to first and second orders when $b \to 1$ and $b \to 2$ respectively [21]. For testing the goodness of fit, the figure of merit (FOM) has been used [22].

$$FOM = \sum_{j_f}^{j_1} \frac{100[y_i - y(x_i)]}{A} \tag{3}$$

where j_f and j_1 are the numbers of the first and last temperature interval ΔT used for curve fitting, Y_i is the intensity in the ith interval obtained from the experiment and $Y(x_i)$ the intensity expected from the model and A, the total area of fitted glow peak between j_f and j_1. FOM values lower than 2.5% show a good fitness to experimental glow curves.

The TL response is highly sensitive to the amount of the impurity ion. So the effect of dysprosium concentration on the TL sensitivity of CaF_2:Dy nanoparticles was studied. As pointed out in section 2.1, the CaF_2 nanoparticles with different concentrations

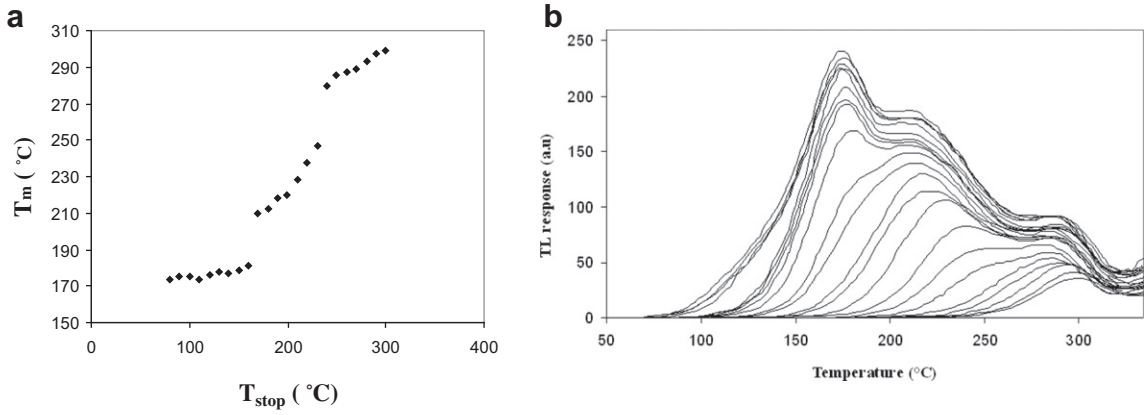

Fig. 5. (a) Variation of temperature of peak maximum, T_m vs. T_{stop}. (b) TL glow curves of the produced nanoparticles following annealing the samples up to different values of T_{stop} from 80–300 °C.

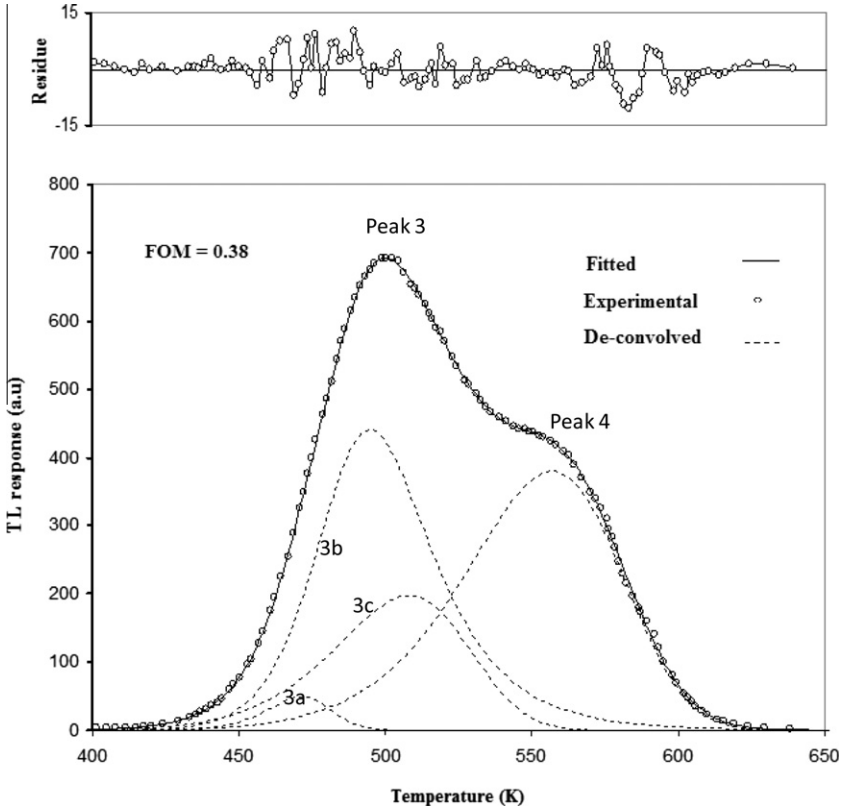

Fig. 6. The high temperature part of the TL glow curve of CaF_2:Dy nanoparticles including the glow peaks3 and 4 along with the de-convolved glow peaks. The glow peak 4 has been separated from the higher temperature peaks by using the thermal cleaning method.

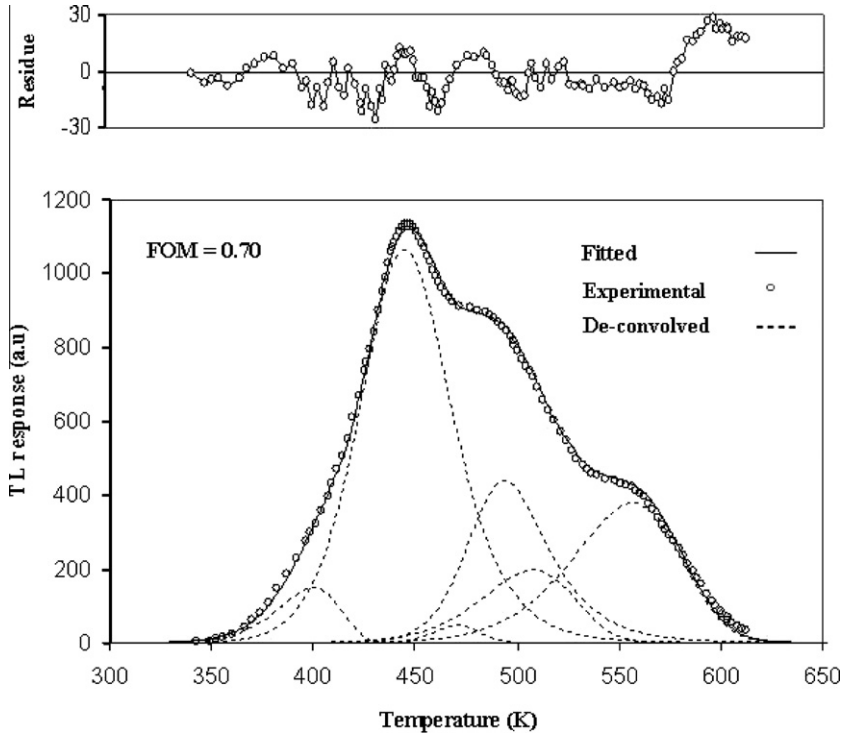

Fig. 7. The experimental whole TL glow curve of the synthesized nanomaterial (open circles) and the deconvolved glow peaks (dashed curves). The TL intensities of the peak components were added to give the whole glow curve obtained from the model (solid curve).The difference between the glow curves obtained from the experiment and the model is shown as the residue at the top of the figure.

of dysprosium impurity can be produced by varying the values of dysprosium nitrate in the synthesis procedure. To obtain the optimum concentration of the Dy impurity, the same masses of the synthesized nanoparticles with different concentrations of Dy

Table 1
TL kinetic parameters of the component glow peaks of the synthesized nanoparticles obtained by the CGCD method.

Peak	b	E(eV)	t_m(K)	I_m(a,u)
1	1.71	1.012	399	156
2	1.86	1.019	442	1042
3(a)	1.35	2.04	471	49
3(b)	2.21	1.72	494	440
3(c)	1.12	1.00	508	197
4	1.10	1.02	556	379

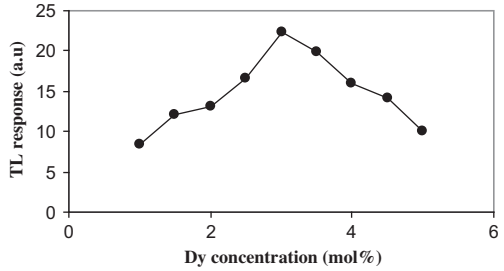

Fig. 8. Variation of the TL response of CaF_2:Dy nanoparticles with concentration of Dy dopant. The optimum sensitivity was achieved at 3 mol% of Dy.

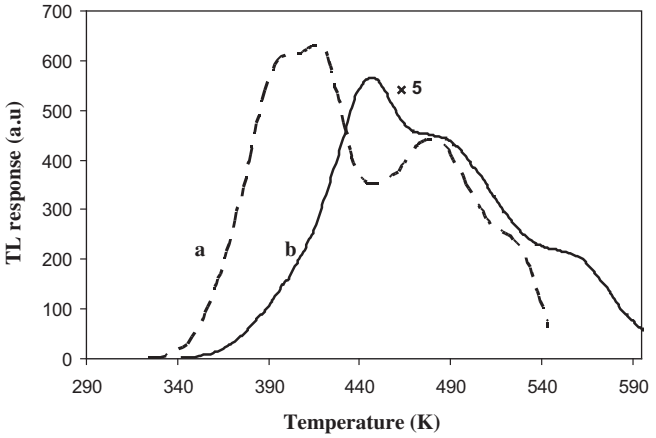

Fig. 9. TL glow curves of commercial CaF_2:Dy (TLD-200) (a) and the synthesized CaF_2:Dy nanoparticles (b) following irradiating the samples with 5 Gy dose from the ^{60}Co gamma source. The TL intensity of nanoparticles was magnified by a factor of 5 for better comparison of the two glow curves.

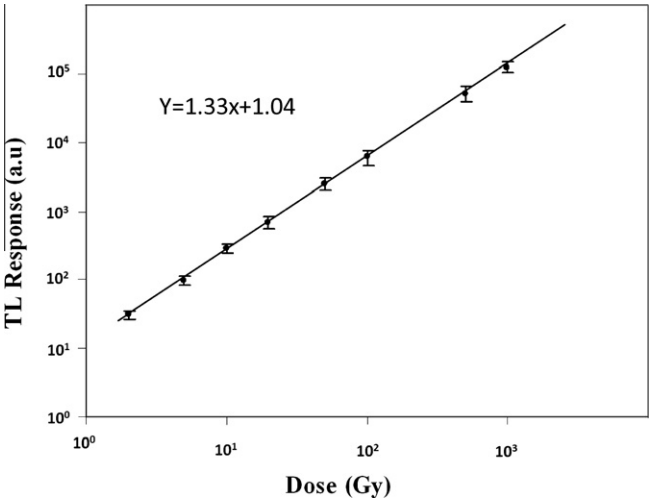

Fig. 10. The TL dose response of CaF_2:Dy nanoparticles in a log–log scale. As is observed, all the data points to a absorbed dose of 1KGy are fairly fitted to a straight line given in the inset with a slope of 1.33.

were annealed followed by irradiation with a specific gamma dose and their TL responses were recorded in the same condition. The results are depicted in Fig. 8. The maximum sensitivity found at approximately 3 mol% of Dy impurity. Also the TL sensitivity of the synthesized CaF_2:Dy nanoparticles were compared with the TLD-200 samples. So, the TLD-200 chips were annealed at 500 °C for 1 h and were irradiated with 5 Gy gamma dose together with the annealed samples of the nanoparticles of the same mass. Then their TL responses were plotted in Fig. 9. It is observed in this figure that the TL response of CaF_2:Dy nanoparticles are around five times lower than that of TLD-200 phosphors. For studying the linearity of dose response, samples of same masses of the CaF_2:Dy nanoparticles were exposed to different doses from ^{60}Co gamma rays and the TL responses for different absorbed doses were recorded. The results are shown in Fig.10. As is seen, all the data points are well fitted to a straight line. Considering the log–log scale in Fig.10, the straight line with a definite slope of 1.33, shows that the dose response is roughly linear to absorbed dose of 1000 Gy. One report demonstrates a linear dose response to about 10^2 Gy for low temperature peaks of TLD-200 [23], while a linear dose response to 6 Gy is observed for this phosphor in another published work [6]. Thus our synthesized CaF_2:Dy nanoparticles show a near linear dose response in a broad range of the absorbed dose compared with its bulk counterpart. The stability of the stored signal at room temperature is an important factor in many applications. Fading of the stored signal befalls due to the loss of electrons from traps and redistribution of traps. Since the stored signal is proportional to both the TL emitted and the radiation exposure, any significant reduction of the stored signal before readout the sample, results in considerable error in estimating the absorbed dose. To study the fading of the stored signal in CaF_2:Dy nanoparticles, the same samples were irradiated with 5 Gy gamma dose and then were stored in dark and subsequently their TL responses were recorded after 0, 1, 7 and 15 days and one month. The results are shown in Fig. 11. The open triangles in Fig. 11(a) show the TL response against the storage time following thermal cleaning of the low temperature peak 1 and the solid triangles show the TL response including the low temperature glow peak. Comparison of the two plots reveals that a reduction of about 7% in the TL response following storage of the samples for 30 days is mainly due to the unstable low temperature peak at 400 K and an ignorable fading results following thermal cleaning of the first glow peak. Also the corresponding TL glow curves with and without the low temperature component are shown as Fig. 11 (b). Fading of TLD-200 chips have been considered by different researchers. Fading of 45% and 12% of the initial signals was reported for the first and second peaks of TLD-200 chips after 35 days storage at room temperature [24]. In addition, a total post-irradiation fade of 19% in the TL response was determined for TLD-200 [25] and less than 25% loss over 30 days reported for this phosphor [6]. It is obvious that the synthesized phosphor have a superior stability of TL response compared to the microcrystalline CaF_2:Dy. Finally, the reusability of this TL material was studied. Thus, the average TL responses of the samples of the same masses following 10 successive cycles of annealing, irradiation with 0.3 Gy of gamma radiation and readout processes were plotted as Fig. 12. As is evident, the TL response is stable after several reuses.

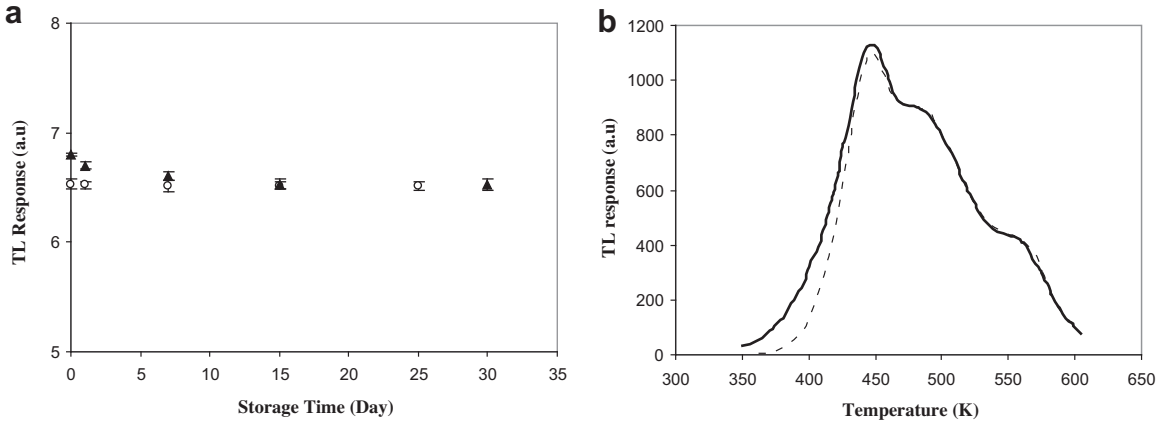

Fig. 11. (a) TL response of CaF_2:Dy nanoparticles against the storage time at room temperature with considering the low temperature peak (solid triangle) and following thermal cleaning of the low temperature peak (open circles). (b) TL glow curves including the low temperature peak at about 400 K (solid line) and after removing this peak by thermal cleaning method (dashed line). The glow curve area without the low temperature peak was observed approximately unchanged with the storage time.

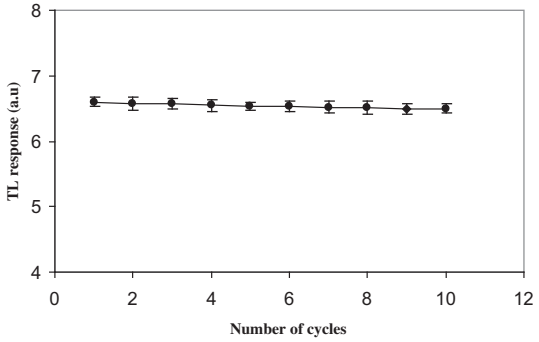

Fig. 12. TL response of CaF_2:Dy nanoparticles for 10 successive cycles of annealing, irradiations and readouts. Error bars show uncertainties originated from readouts of seven samples.

4. Conclusions

The CaF_2:Dy nanoparticles were synthesized by the hydrothermal method. The $T_m - T_{stop}$ curve indicated that the glow peak 3 has a complex nature and further investigations revealed that it is a superposition of three closely lying glow peaks. The sensitivity of the produced CaF_2:Dy nanostructure is less than that of its microcrystalline counterpart, however, its linear region of TL dose response extends over very high absorbed doses compared with its bulk equivalent. Furthermore, the raising part of the glow curve of the synthesized nanoparticles lies at higher temperatures compared with the microcrystalline CaF_2:Dy. This property resulted in very low fading of the prepared nanocrystalline. The fading of the synthesized nanoparticles is mainly due to the small satellite unstable glow peak at 127 °C. Thus applying a post-irradiation annealing up to about 125 °C make the TL signal to be almost stable against the storage time. Considering the proper dosimetric features of this phosphor, The synthesized CaF_2:Dy nanocrystalline is highly recommended for high dose dosimetry.

Acknowledgements

The research council of the University of Kashan is gratefully acknowledged for its support of this work.

References

[1] B. Ben Shachar, Y. Laichter, U. German, G. Weiser, An improved energy compensating holder for CaF_2:Dy–TLD crystals used for environmental measurements, Radiat. Prot. Dosim 12 (4) (1986) 333–337.
[2] S.W.S. McKeever, M. Moscovitch, P.D. Townsend, TL Dosimetry Materials: Properties and Uses, Nuclear Technology Publishing, Ashford, 1995.
[3] T.K. Wang, P.C. Hsu, P.S. Weng, Application of TLD-200 dosimeters to the discrimination of α, β and γ radiation, Radiat. Prot. Dosim. 16 (3) (1986) 225–230.
[4] J.B. Dielhof, A.J.J. Bos, J. Zoetelief, J.J. Broerse, Sensitivity of CaF_2 thermoluminescent materials to fast neutrons, Radiat. Prot. Dosim 23 (1/4) (1988) 405–408.
[5] F. Hasan, S. Charalambous, The thermoluminescence behavior of CaF_2:Dy (TLD-200) for low up to high doses, J. Phys. C: Solid State Phys. 16 (1983) 5921–5928.
[6] W. Binder, J.R. Cameron, Dosimetric properties of CaF_2:Dy, Health Phys. 17 (1969) 613–618.
[7] A.N. Yazici, R. Chen, S. Solak, Z. Yegingil, The analysis of thermoluminescent glow peaks of CaF_2:Dy (TLD-200) after β- irradiation, J. Phys. D Appl. Phys. 35 (2002) 2526–2535.
[8] N. Salah, P.D. Sahare, S.P. Lochab, P. Kumar, TL and PL studies on $CaSO_4$:Dy nanoparticles, Radiat. Meas. 41 (2006) 40–47.
[9] A. Vij, S.P. Lochab, R. Kumar, N. Singh, Thermoluminescence response and trap parameters determination of gamma exposed Ce doped SrS nanostructures, J. Alloys Compd. 490 (2010) L33–L36.
[10] G. Sharma, S.P. Lochab, N. Singh, Thermoluminescence characteristics of gamma irradiated CaS:Ce nanophosphors, J. Alloys Compd. 501 (2010) 190–192.
[11] M. Zahedifar, M. Mehrabi, Thermoluminescence and photoluminescence of cerium doped $CaSO_4$ nanosheets, Nucl. Instr. Meth. B 268 (2010) 3517–3522.
[12] M. Zahedifar, M. Mehrabi, S. Harooni, Synthesis of $CaSO_4$: Mn nanosheets with high thermoluminescence sensitivity, Appl. Radiat. Isot. 69 (2011) 1002–1006.
[13] S.C. Prashantha, B.N. Lakshminarasappa, B.M. Nagabhushan, Photoluminescence and thermoluminescence studies of Mg_2SiO_4: Eu^{+3} nano phosphor, J. Alloys Compd. 509 (2011) 10185–10189.
[14] N. Salah, Nanocrystalline materials for the dosimetry of heavy charged particles: a review, Radiat. Phys. Chem. 80 (2011) 1–10.
[15] C. Pandurangappa, B.N. Lakshminarasappa, B.M. Nagabhushana, Synthesis and characterization CaF_2 nanocrystals, J. Alloys Compd. 489 (2010) 592–595.
[16] Z. Xia, P. Du, Synthesis and upconversion luminescence properties of CaF_2: Yb, Er nanoparticles obtained from SBA-15 template, J. Mater. Res. 25 (10) (2010) 12.
[17] B.C. Hong, K. Kawano, Syntheses of CaF_2:eu nanoparticles and the modified reducing TCRA treatment to divalent Eu ion, Opt. Mater. 30 (2008) 952–956.
[18] M. Zahedifar, E. Sadeghi, Z. Mohebbi, Synthesis and thermoluminescence characteristics of Mn doped CaF_2 nanoparticles, Nucl. Inst. Meth. B 274 (2012) 162–166.
[19] T. Vilaithong, S. Wanwilairat, M. Rhodes, W. Hoffmann, T. Messarius, High resolution emission spectra of TL materials, Radiat. Prot. Dosim. 100 (1–4) (2002) 211–216.
[20] G.G. Kitis, J.M. Gomez Ros, J.W.N. Tuyn, Thermoluminescence glow curve deconvolution functions for first, second and general orders of kinetics, J. Phys. D:Appl. Phys. 31 (1998) 2636–2641.
[21] A.J.J. Bos, Theory of thermoluminescence, Radiat. Meas. 41 (2007) 45–56.

[22] H.G. Balian, N.W. Eddy, Figure of merit (FOM), an improved criterion over the normalized chi squared test for assessing goodness-of-fit of gamma-ray spectra peaks, Nucl. Inst. Meth. 145 (1977) 389–393.
[23] V.E. Kafadar, A.N. Yazici, R.G. Yildirim, The effects of heating rate on the dose response characteristics of TLD-200, TLD-300 and TLD-400, Nucl. Inst. Meth. B 267 (2009) 3337–3346.
[24] C. Bacci, C. Furetta, B. Rispoli, G. Roubaud, J.W.N. Tuyn, The effect of storage temperature on the thermoluminescence response of some phosphors, Radiat. Prot. Dosim. 25 (1) (1988) 43–48.
[25] J.A. Harvey, N.P. Haverland, K.J. Kearfott, Characterization of the glow-peak fading properties of six common thermoluminescent materials, Appl. Radiat. Isot. 68 (2010) 1988–2000.